Journal of Materials Chemistry

Cite this: J. Mater. Chem., 2012, 22, 9853

www.rsc.org/materials

PAPER

Boron carbide nanowires: low temperature synthesis and structural and thermal conductivity characterization†

Zhe Guan,[a] Timothy Gutu,[a] Juekuan Yang,[b] Yang Yang,[b] Alfred A. Zinn,[c] Deyu Li*[b] and Terry T. Xu*[a]

Received 28th September 2011, Accepted 8th March 2012
DOI: 10.1039/c2jm14857a

Boron carbide nanowires, a promising class of high temperature thermoelectric nanomaterials, are synthesized by co-pyrolysis of diborane and methane in a low pressure chemical vapor deposition system *via* the vapor–liquid–solid growth mechanism. Nickel and iron are effective catalytic materials. The synthesis is realized at relatively lower temperatures, with 879 °C as the lowest one. Electron microscopy analysis shows that the as-synthesized nanowires have diameters between 15 and 90 nm and lengths up to 10 μm. The nanowires have single crystalline boron carbide cores and thin amorphous oxide sheaths. Both transverse faults and axial faults with fault planes as $\{101\}_H$-type are observed, which could provide additional measures to tune the nanowire transport properties for better thermoelectric performance. Measurement of individual boron carbide nanowires reveals that the thermal conductivity is diameter-dependent, which indicates that boundary scattering still provides an effective approach to reduce the wire thermal conductivity for enhanced thermoelectric performance.

Introduction

Boron carbides are strong candidates for high temperature thermoelectric power generation.[1–5] They exhibit unusual transport properties such as thermally activated electrical conductivity, anomalously large Seebeck coefficients (as high as >300 $\mu V\ K^{-1}$), and extremely slow thermal diffusion despite their very high sound velocity.[3] The dimensionless thermoelectric figure-of-merit (ZT) on the order of one was reported, whereas $ZT \gg 1$ has also been predicted at high temperatures.[1]

The extraordinary thermoelectric properties of boron carbides are believed to emerge from their unique crystal structures.[3,6,7] Boron carbides are compositionally disordered materials that exist as a single rhombohedral phase compound in a wide range of compositions: from $B_{10.4}C$ (8.8 at% C) to B_4C (20 at% C).[7,8] Within a rhombohedral lattice, eight 12-atom icosahedra locate at the corners and one 3-atom chain occupies the longest diagonal of the rhombohedron.[7] Compositional disorder is represented by the replacement of boron atoms with carbon atoms at several locations. For example, the icosahedra can be composed of either twelve boron atoms (B_{12}) or eleven boron atoms and one carbon atom ($B_{11}C$), whereas the 3-atom chain can be B–B–B, C–B–C, or C–B–B.[3,4,9,10] The variation of carbon content within the homogeneity range could lead to the presence of highly concentrated intrinsic structural defects in boron carbides (*e.g.*, ~9.3% in $B_{13}C_2$).[11] Such defects, in the form of incomplete occupation of specific sites or of antisite defects, could greatly influence relevant transport properties.[11] Two main models of charge transport in boron carbides, the bipolaron model by Emin[3] and the defects-based model by Werheit,[6,11] have been debated for many years. So far, most transport measurements on boron carbides were on polycrystalline specimens prepared by melting or hot pressing.[5,12,13] The existence of grain boundaries, impurities and other defects always complicated experimental results, making correlation between experimental results and theoretical prediction difficult. Thus, it is necessary to prepare single crystalline boron carbides for fundamental studies.

Additionally, although promising thermoelectric properties were observed for boron carbides, improved thermoelectric performance (*i.e.*, higher ZT) is inevitably needed to facilitate the realization of future high-efficiency thermoelectric devices. It is from recent advances that low-dimensional materials such as quantum dots, nanowires and thin films provide new opportunities to achieve higher ZT.[9,10,14] Because of both a tuned electron density of states induced by quantum confinement effects for enhanced thermoelectric power factor and increased phonon boundary or interface scattering for reduced thermal conductivity, enhanced thermoelectric performance in low-dimensional nanomaterials as compared to their counterpart bulk materials can be realized. Most recent publications show that thermal

[a]*Department of Mechanical Engineering and Engineering Science, The University of North Carolina at Charlotte, Charlotte, NC 28223, USA. E-mail: ttu@uncc.edu*
[b]*Department of Mechanical Engineering, Vanderbilt University, Nashville, TN 37235, USA. E-mail: deyu.li@vanderbilt.edu*
[c]*Advanced Technology Center, Lockheed Martin Space System Company, Palo Alto, CA 94304, USA*

† Electronic supplementary information (ESI) available: Additional description of boron carbide 1D nanostructures of different morphologies other than that reported in the main paper, the histogram of diameters of as-synthesized boron carbide nanowires, and issues on recognizing twinned structures during TEM examination. See DOI: 10.1039/c2jm14857a

conductivity reduction is especially easy to achieve in nanostructured materials such as various nanowires.[15–18] Thus, it is of great interest to synthesize low-dimensional boron carbides and explore whether they exhibit better thermoelectric performance.

Boron carbide low-dimensional nanostructures have been synthesized by several research groups.[19] The most common method is carbothermal reduction, in which solid precursors of boron, boron oxide, and carbon are mixed and reacted at high temperatures between 1100 and 1800 °C for several hours.[20–26] Most synthesized nanostructures were claimed to be rhombohedral B_4C, whereas metastable orthorhombic B_8C was also reported.[27] Mechanical,[26] photoluminescence,[24] and field emission[25] properties of boron carbide nanowires were studied, whereas transport properties have not been explored. In this paper, we report on the synthesis of crystalline boron carbide nanowires by co-pyrolysis of diborane (B_2H_6) and methane (CH_4) in a low pressure chemical vapor deposition (LPCVD) system at temperatures below 1000 °C. The CVD-based method is energy efficient and cost effective. The lowest synthesis temperature was found to be 879 °C, which is significantly lower than those reported for carbothermal reduction. The reaction time (*e.g.*, 45 minutes to produce ~5 μm long nanowires) is also shorter than that for carbothermal reduction. The as-synthesized nanowires were characterized to have single crystalline boron carbide cores and thin amorphous oxide sheaths. Planar faults of different morphology, including both transverse faults and axial faults, were observed and thoroughly characterized. These boron carbide nanowires allow for studies of the effects of crystalline defects and boundaries on transport properties at the nanoscale, and could lead to further enhanced thermoelectric performance. To verify that the nanowire surface still plays an important role in phonon transport, the thermal conductivity of different diameter individual boron carbide nanowires was measured. Results show that the nanowire thermal conductivity reduces for smaller diameter wires, which indicates that phonon-boundary scattering is still an important factor in determining the phonon mean free path even for the complex crystalline structure with multiple planar faults. The measured room temperature thermal conductivity of a 55 nm diameter nanowire is 3.78 W m^{-1} K^{-1}, which is eight times lower than that of bulk single crystalline B_4C.

Experimental

Boron carbide one-dimensional (1D) nanostructures were synthesized by co-pyrolysis of B_2H_6 and CH_4 at elevated temperatures in a LPCVD system. Detailed description of the LPCVD system can be found elsewhere.[28,29] Typical synthesis conditions are described here, whereas conditions used for controlled experiments (*e.g.*, variation of reaction temperatures, reaction time, *etc.*) and their effects on the synthesized nanowires are discussed in the next section.

Silicon (Si) wafers with one micron thick thermally grown silicon dioxide (SiO_2) purchased from University Wafer were cut into small pieces (10 mm × 25 mm). These SiO_2/Si substrates first went through a three-step cleaning process, including (i) ultrasonic cleaning by certified ACS grade acetone and methanol (Branson Ultrasonic Cleaner; 70 W, 3 minutes), (ii) blow drying by compressed nitrogen, and (iii) oxygen plasma cleaning (Kurt J Lesker: Plasma-Preen 862; oxygen flow rate: 1.94 standard cubic feet per hour, 425 W, 3 minutes). The cleaned substrates were then coated with a 2 nm thick nickel (Ni) thin film using magnetron sputtering (Denton Vacuum: Desk IV TSC). The coated substrates were subsequently loaded into a quartz boat, and placed in a desired position in the quartz tube of the LPCVD system. The whole system was first evacuated to a pressure of ~7 mTorr, after which the quartz tube was ramped up to 1050 °C (center position temperature measured outside the quartz tube by a thermocouple) in 50 minutes. A constant flow of 15 sccm (standard cubic centimetres per minute) Ar (Linde; 99.999% UHP) was maintained during the whole experiment. To synthesize boron carbide 1D nanostructures, 15 sccm B_2H_6 (Voltaix; 5% ultrahigh purity B_2H_6 in research grade Ar) and 15 sccm CH_4 (Linde Gas; compressed methane) were introduced to the quartz tube for 45 minutes at 1050 °C. The typical reaction pressure was ~440 mTorr. After reaction, the quartz tube was cooled down to room temperature naturally in ~5 hours. The substrates were then taken out and characterized by scanning electron microscopy (SEM; JEOL JSM-6480) and transmission electron microscopy (TEM; JEOL JEM-2100 LaB_6 microscope) including electron diffraction, high resolution TEM (HRTEM) and energy dispersive X-ray spectroscopy (EDS; Oxford Instruments: with a super atmospheric thin window X-ray detector which is capable of detecting boron).

Results and discussion

Due to the unique combination of temperature gradient and gas distribution in our reaction chamber, crystalline boron-based 1D nanostructures with various morphologies could be synthesized (see ESI, S1†). For example, α-tetragonal boron ($B_{50}C_2$) nanoribbons were produced in the temperature range of 630–750 °C. Tapered short boron carbide nanostructures (~2 μm in length) were produced in the temperature range of 908–931 °C. Long and thin boron carbide nanowires were found in the 964–977 °C temperature zone that was about 15 mm long. The synthesis and characterization of these long boron carbide nanowires, which are great samples for thermoelectric property studies, are the focus of this paper.

Characterization of as-synthesized nanowires

Fig. 1a is an SEM image of as-synthesized nanowires having diameters between 15 and 90 nm and lengths up to 10 μm (the histogram of diameters can be found in the ESI, S2†). In order to find out detailed crystallographic information of these nanowires, more than ninety of them were studied by TEM. Typical results are presented in Fig. 1b. Inset I in Fig. 1b is a low magnification TEM image of a part of a nanowire. The catalytic material at the tip of the nanowire is clearly revealed. The HRTEM image (Fig. 1b) of the area enclosed by the black rectangle in inset I shows that the nanowire has a single crystalline core and a 0.5–2 nm thick amorphous sheath. The image also reveals the existence of planar defects such as twins and stacking faults in the nanowire. Inset II is the corresponding selected area electron diffraction pattern recorded along the $[12\bar{1}]_h$ zone axis. (Note: the subscript *h* refers to the hexagonal representation.) The streaks in the diffraction pattern further

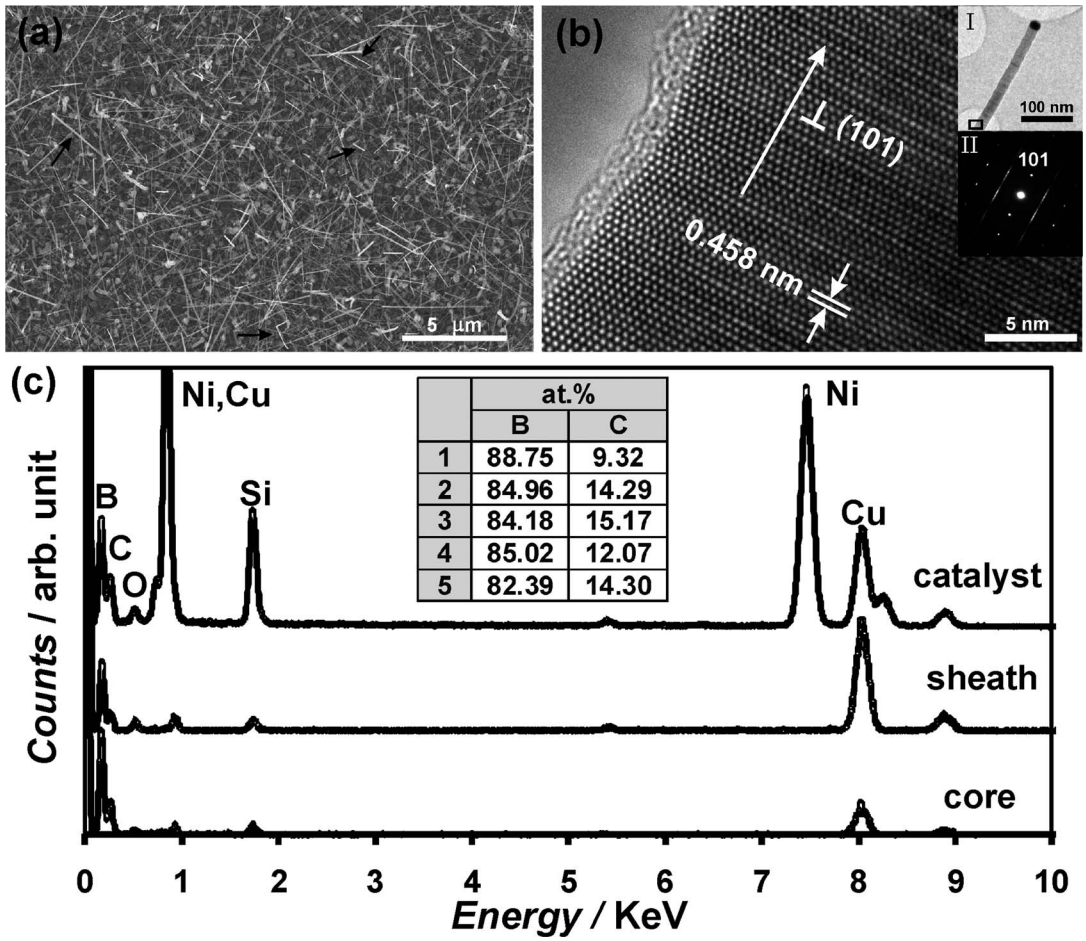

Fig. 1 Materials characterization of as-synthesized nanowires. (a) An SEM image shows both straight and kinked nanowires (pointed by black arrows). (b) TEM results show the nanowire has a single crystalline core and a 0.5–2 nm thick amorphous oxide sheath. The preferred growth direction of the nanowire is perpendicular to $(101)_h$ planes. (c) EDS results show the compositional information within the core, sheath and catalyst of a nanowire. The inset is a summary of atomic percentage of B and C in five different nanowires.

confirm the existence of planar defects in the nanowire. On the basis of the HRTEM imaging and electron diffraction pattern analysis, the nanowire was found to have a rhombohedral boron carbide lattice. As mentioned before, boron carbide is a solid solution with carbon composition varying between 8.8 and 20 at %. According to the Joint Committee on Powder Diffraction Standards (JCPDS) database, there are at least seven rhombohedral boron carbides such as B_4C, $B_{10}C$ and $B_{13}C_2$. These boron carbides with different chemical formulae share identical crystal structure and similar lattice parameters of variation less than 1.5%.[30] Based on the TEM results, it is difficult to accurately distinguish phases between various boron carbides. However, the calculated lattice constants for this particular nanowire are closer to values for $B_{13.7}C_{1.48}$ according to the JCPDS 01-071-0363. The preferred growth direction of the nanowire was found to be perpendicular to the $(101)_h$ plane. (Note: the subscript *h* refers to the hexagonal representation. $(101)_h$ is equivalent to $(100)_r$, where *r* refers to the rhombohedral representation.) Among all nanowires analyzed, approximately 75% were grown perpendicular to the $(101)_h$ plane. Fig. 1c reveals the EDS results of compositional information in the core, sheath and tip of the nanowire. The existence of B, C, O and Si was found in both the core and sheath. (Note: the Cu signal comes from the supporting Cu grid and is not a component of the nanowire.) The higher O : B (or O : C) ratio observed from the sheath indicates that the periphery of the nanowire is rich in O. The inset shows the results from semi-quantitative analysis of atomic percentage of B and C in cores of five nanowires. Variation of compositions among nanowires is revealed, although all nanowires have the rhombohedral lattice. This observation is consistent with the fact that boron carbide is a solid solution with carbon atomic percentage varying between 8.8 and 20% and cannot be described by a simple fixed chemical formula (although B_4C is being widely used as the chemical formula of boron carbide). The catalytic material is composed of B, C, O, Ni and Si. A very small amount of Si exists in both the core and the sheath. The source of Si was discussed in our previous publication.[31] In general, the Si might come from the SiO_2/Si substrates, quartz boats and quartz tubes used for LPCVD synthesis.

Controlled synthesis experiments

Other than the standard experiment mentioned in the Experimental section (*i.e.*, use of Ni as the catalytic material, 15 sccm

B_2H_6 + 15 sccm CH_4 + 15 sccm Ar gas flow, 1050 °C furnace center temperature, 45 minutes reaction time), a set of controlled synthesis experiments were carried out to explore the growth mechanism and optimize the growth conditions of boron carbide nanowires.

(i) Catalytic materials. Fig. 2a and b illustrate that growth of nanowires occurred only when catalytic materials such as Ni were used. As revealed by the aforementioned TEM analysis, Ni was commonly found at tips of nanowires. This result indicates that the growth of these nanowires can be attributed to the vapor–liquid–solid (VLS) mechanism.[32] Both Ni and Fe were found to be effective catalytic materials to grow boron carbide nanowires.

(ii) Reaction time. With other parameters (*i.e.*, catalytic material used, reaction temperature and gas flow rate) unchanged, the reaction time was varied from 5 to 120 minutes. No growth of nanowires was observed when the reaction time is less than 15 minutes. Between 15 and 80 minutes, a longer reaction time led to more and longer nanowires (Fig. 2c and d). However, further increasing the reaction time to 120 minutes mainly resulted in coarsening of nanowires, instead of more and longer nanowires. The optimal reaction time was found to be 80–90 minutes, producing nanowires with a mean diameter of ~50 nm and an average length of 10 μm.

(iii) Reaction temperature. The center temperature of the furnace was varied from 900 to 1050 °C with an interval of 50 °C. Growth of nanowires was not observed until the center temperature was greater than or equal to 950 °C. When the center temperature was set as 950 °C (Fig. 2e), nanowires were found in the 879–885 °C temperature zone region. When the center temperature was set as 1050 °C (Fig. 2f), nanowires were observed in the 964–977 °C region. Independent of the prescribed furnace center temperatures, the growth region is always approximately 1.5 cm long. However, a higher center temperature could lead to production of more and longer nanowires. To the best of our knowledge, the observed growth temperature (min. 879 °C) in this study is the lowest temperature used to synthesize crystalline rhombohedral boron carbide nanowires by vapor-based and carbothermal reduction techniques.[19]

(iv) Ratio between B_2H_6 and CH_4. The effect of amount of gas precursors was studied by changing the flow ratio between B_2H_6 and CH_4. Nanowires can be synthesized when the ratio of flow rate between B_2H_6 and CH_4 is less than five. For instance, keeping the flow rate of B_2H_6 as 15 sccm, the growth of nanowires was stopped when the flow rate of CH_4 was less than 3 sccm. As shown in Fig. 2g and h, a higher CH_4 flow (*i.e.*, lower B_2H_6/CH_4 ratio) can facilitate the growth of boron carbide nanowires.

(v) Materials of the substrate and the reaction tube. When the substrate was changed from SiO_2/Si to sapphire and the reaction tube was simultaneously changed from quartz to alumina, Al-doped boron carbide nanowires can be synthesized. As discussed in our previous report,[31] the pyrolysis of B_2H_6 might yield highly reactive boron and hydrogen, interacting with substrate and reaction tube and producing gas phase Si-containing species (such as SiH_x radicals, $x = 1$ to 3) or Al-containing species. These Si (or Al)-containing species could in turn serve as dopants and produce doped boron carbide nanowires.

Planar defects in as-synthesized nanowires

The crystal structure of boron carbide can be viewed as a rhombohedral distortion of the cubic close packing (ccp) of B_{12} or

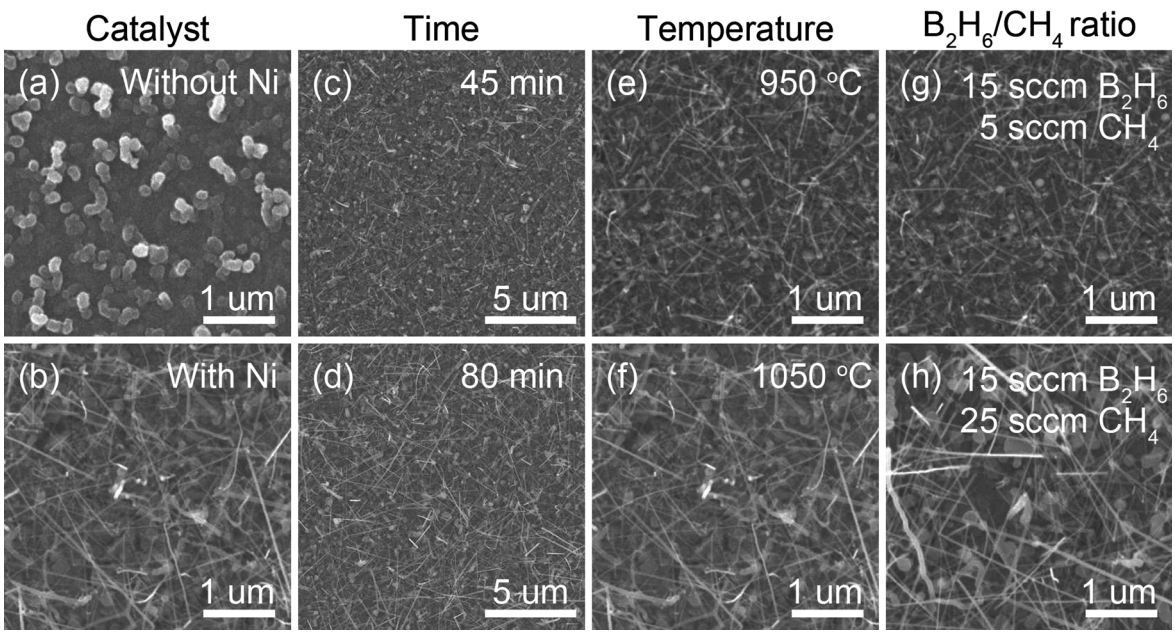

Fig. 2 Results of controlled synthesis experiments illustrate effects of catalytic materials, reaction time, temperature and flow rate ratio between B_2H_6 and CH_4 on growth of boron carbide nanowires.

$B_{11}C$ icosahedra.[7] The {100} planes of the rhombohedral cell are considered as the close-packed planes in the ccp arrangement. They are stacked by a sequence of …ABCABC… as illustrated in Fig. 3a. If this normal stacking sequence is disturbed, planar defects such as stacking faults and twins can be formed. Due to its relatively lower stacking fault energy (75 ergs cm^{-2}),[33] twins and stacking faults are commonly observed in bulk boron carbide, such as sintered samples[34–36] and boron carbide particle-reinforced metal matrix composites.[37] For example, a high density of $\{101\}_h$-type twins and stacking faults was observed in hot-pressed $B_{13}C_2$ samples.[35] A follow-up simulation work on HRTEM imaging showed that the twin plane passes through the center of the icosahedron instead of being translated half-way between the rows of icosahedra parallel to $(101)_h$.[36] The introduction of a $(101)_h$ twin plane through the icosahedron distorts the inter- and intra-icosahedral bonding, which could lead to increased bipolaron hopping and affect relevant transport properties.[36] Twins formed in bulk boron carbide are usually deformation twins.[34,37] Their formation can be partly attributed to the localized stress state induced during complicated synthesis processes (*e.g.*, milling, hot pressing).[37] Observations of twins and stacking faults have also been reported for some boron carbide low-dimensional nanostructures, such as whiskers,[20,38,39] nanowires,[40–42] platelets,[20] and sheets.[22] However, no detailed and systematic documentation such as those discussed below can be found.

In the present work, more than ninety nanowires were carefully examined by TEM. To reveal whether the nanowire has structural defects or not, wide angle of tilting was done on each nanowire during TEM examination (see ESI, S3†). 75% of examined nanowires were found to have $\{101\}_h$-type planar faults. Based on the geometrical relationship between the fault plane and the preferred growth direction of the nanowire, the faults can be categorized into transverse faults (fault plane $\perp$ nanowire preferred growth direction) and axial faults (fault plane $\parallel$ nanowire preferred growth direction). Fig. 3b and c show a nanowire with transverse faults in which variable width twins and stacking faults are revealed. The faults have atomic sharp boundaries, indicating they are not deformation faults but growth faults.[37] The white line helps the visualization of the zigzag facets on the wire side surface. These facets are $(1\bar{1}\bar{1})_h$ planes. The marked rotation angle is approximately 146°, twice

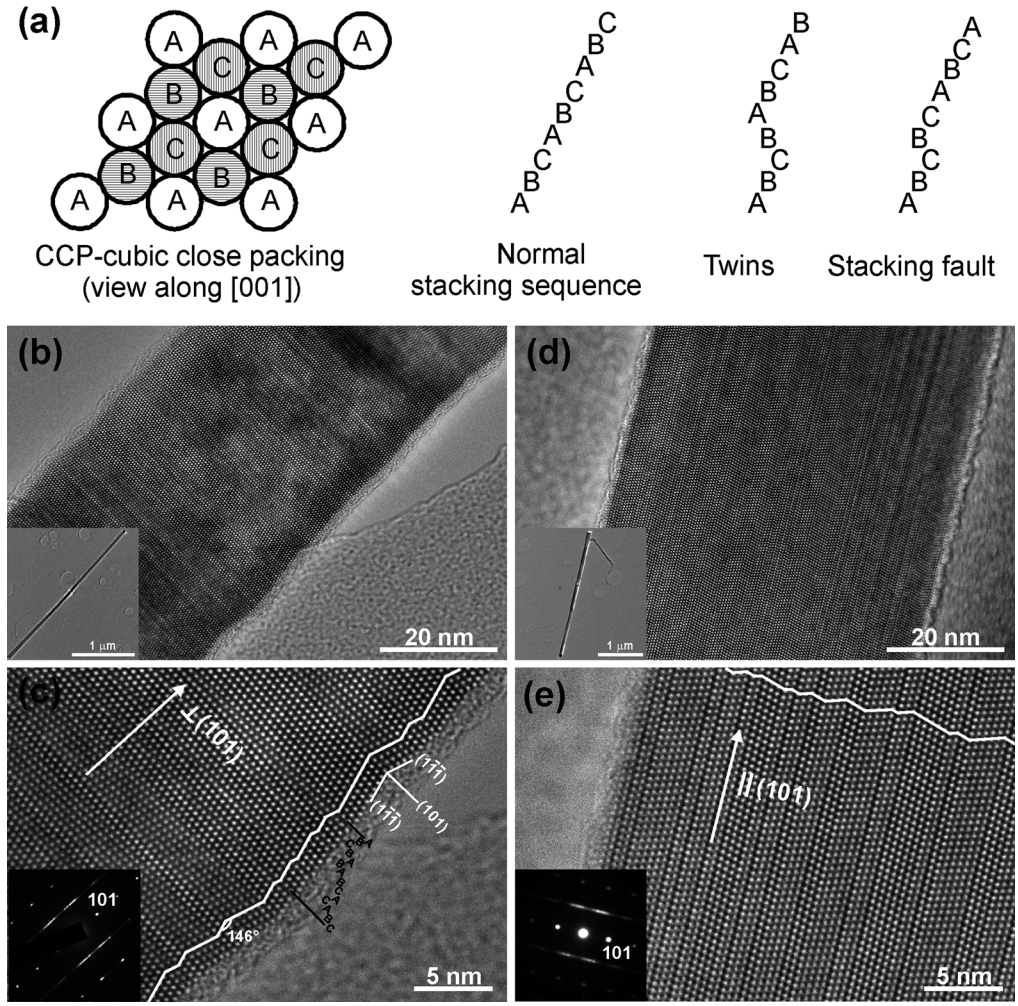

Fig. 3 Study of planar defects in as-synthesized nanowires. (a) Schematic drawings show the ccp arrangement for a rhombohedral boron carbide structure, normal stacking sequence, twins and stacking faults induced by disordered stacking. (b and c) TEM results show the existence of transverse faults. (d and e) TEM results show the existence of axial faults.

the interplanar angle between $(101)_h$ and $(1\bar{1}\bar{1})_h$ planes (=73°). The two crystallographic equivalent planes, $(101)_h$ and $(1\bar{1}\bar{1})_h$, have the highest planar density in the rhombohedral lattice. Therefore, they have the lowest surface energy and can be energetically more favourable to form during growth. For a portion of the nanowire, the disturbance of stacking sequence is labelled. The new stacking sequence is ABCBABABCA/CABC where the representative microtwinned region is underlined and one intrinsic stacking fault is illustrated by /. Fig. 3d and e show a nanowire with axial faults. Similar to the aforementioned transverse faults, these axial faults consisted of variable-width twins and stacking faults. The side surfaces are $(101)_h$ planes. No clear five-fold cyclic twinning structures as reported previously for boron suboxide[43] and boron carbide nanowires[42] were observed in our nanowires. Approximately 30% of examined faulted nanowires were found to have axial faults.

At the current stage, growth mechanisms of these faulted nanowires are not clear and need further studies. The growth mechanism of nanowires with transverse faults might be similar to the model developed for the growth of InP twinned superlattice nanowires.[44] In that model, the distortion of the catalyst droplet in response to the evolution of the cross-sectional shape of the nanowire affiliates the growth of transverse twins.[44] Similar shape variation of catalysts was observed in the present work and is currently being analyzed. The growth model for nanowires with axial faults might be attributed to a VLS-assisted twin-plane reentrant edge (TPRE) mechanism.[45,46] The TPRE mechanism has been used to explain the growth of boron oxide nanoplatelets[46] and five-fold boron carbide nanowires.[45] In addition, we observed that defects in catalysts can be transferred to nanowires and lead to the growth of nanowires with axial faults.

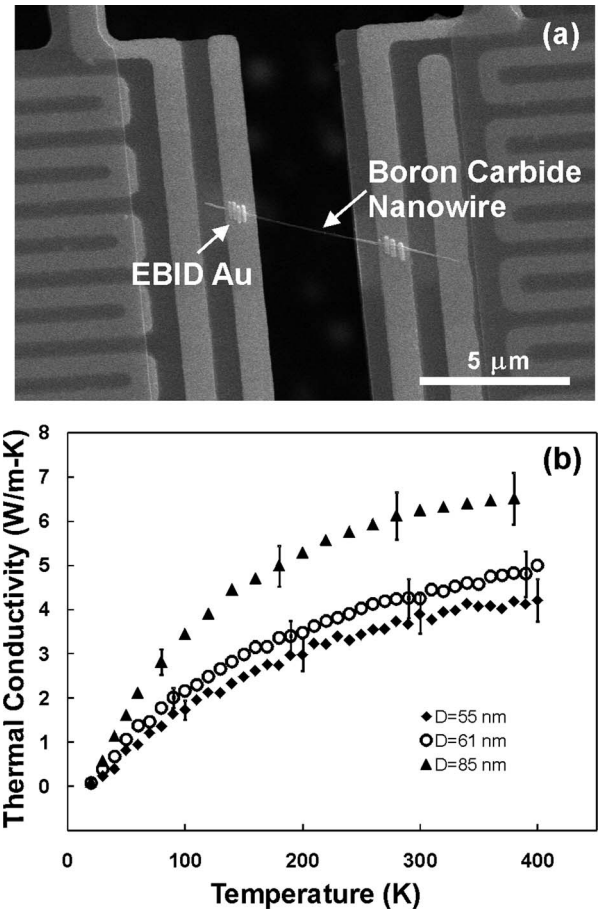

Fig. 4 (a) A boron carbide nanowire of 55 nm diameter on a suspended microdevice for measurement of its thermal conductivity. (b) Measured thermal conductivities of three boron carbide nanowires.

Thermal conductivity measurements

As mentioned in the Introduction, even though both electron band structure manipulation and thermal conductivity reduction in nanostructured materials have been predicted to enhance the thermoelectric figure-of-merit ZT, most experimentally observed ZT enhancement comes from thermal conductivity reduction due to phonon scattering at nanostructure surfaces and interfaces. For the synthesized boron carbides, which have very complex crystalline structures with multiple planar defects such as twins and stacking faults, it is of great interest to see whether their thermal conductivity is still lower than the corresponding bulk value. This critical information will help to determine whether these nanowires will possess an advantage over bulk materials for thermoelectric applications.

In order to see whether phonon-boundary scattering still plays an important role in determining the thermal conductivity of the as-synthesized boron carbide nanowires, thermal conductivity measurements of individual boron carbide nanowires using a unique measurement technique were performed.[47,48] Fig. 4a shows an SEM micrograph of an individual boron carbide nanowire bridging the two suspended membranes of a microdevice with integrated microheaters, thermometers, and electrodes for property characterization. To reduce the contact thermal resistance between the nanowire sample and the suspended membranes, electron beam-induced deposition (EBID) was used to locally deposit some gold at the two wire–membrane contacts.

Fig. 4b shows the measured thermal conductivities of three boron carbide nanowires of different diameters, 55 nm, 61 nm, and 85 nm. It can be clearly seen that as the wire diameter reduces, the thermal conductivity decreases. The clear diameter dependence of the thermal conductivity suggests that even significant amounts of structural defects such as twins and stacking faults exist in these nanowires, phonon-boundary scattering at the nanowire surface still plays an important role in determining the nanowire thermal conductivity. One possible reason for this is that because of the low group velocity of optical phonons and the complex crystalline structures of the boron carbide nanowires, which can effectively scatter high frequency phonons, thermal transport in these boron carbide nanowires heavily relies on low to medium frequency phonons. These low to medium frequency phonons, while not very sensitive to the atomic level defects, are diffusely scattered at the nanowire surface that has a rough oxide sheath, which leads to reduced thermal conductivities for smaller wires. The thermal conductivities of all three wires increase monotonically till 400 K without showing the signature of Umklapp scattering, indicating that the phonon Umklapp scattering is not strong enough in the measurement temperature range to show its signature.

It is worth noting that the thermal conductivity of boron carbides is a strong function of carbon contents. Moreover, thermal conductivity of single crystalline boron carbides could be more than twice higher than the corresponding values of polycrystalline samples.[12] At room temperature, the thermal conductivity of the 55 nm diameter nanowire is 3.78 W m^{-1} K^{-1} (average of the three values at 290, 300 and 310 K), which is about eight times smaller than the bulk value of ~30 W m^{-1} K^{-1} for single crystalline B_4C.[12] In addition, this value is about 50% lower than that for polycrystalline boron carbide with similar carbon contents (*e.g.*, 9–15 at% of carbon), which is ~7 to 12 W m^{-1} K^{-1} at 300 K.[49] Considering that the reported thermal conductivity of bulk samples in this carbon content range is all from polycrystalline samples, the thermal conductivity reduction could be more significant if compared with the values of single crystalline bulk boron carbides of similar carbon content. The lower thermal conductivity of the nanowires and the clear diameter dependence indicate that even with very complex crystalline structures and multiple planar defects, the nanowire surface still plays an important role in phonon transport in these nanowires. Therefore, these nanowires, with reduced thermal conductivity, could be strong candidates for high temperature thermoelectric energy conversion.

Conclusions

In summary, low temperature synthesis of boron carbide nanowires was realized by co-pyrolysis of B_2H_6 and CH_4 in a LPCVD system. Compared to widely used carbothermal synthesis of boron carbide nanowires, the CVD-based method is more energy efficient since it requires much lower reaction temperature and shorter reaction time. The minimum synthesis temperature was found to be 879 °C, which is among the lowest ones reported in the literature. The as-synthesized nanowires were characterized to have single crystalline boron carbide cores and thin (0.5–2 nm) amorphous oxide sheaths. $\{101\}_h$ (equivalent to $\{100\}_r$)-type planar faults such as variable width twins and stacking faults were observed. These faults can be further categorized into transverse faults and axial faults, depending on the geometrical relationship between the fault plane and the preferred growth direction of the nanowire. Although growth of these boron carbide nanowires can be generally attributed to the VLS mechanism, exact growth models for the two categories of planar faults are not clear and need further investigation. Nevertheless, these faulted nanowires with extensive twin boundaries are great candidates for studying and exploring transport properties. Measured thermal conductivities of individual as-synthesized boron carbide nanowires show significantly reduced values compared to the reported thermal conductivities of bulk boron carbides. The thermal conductivity also shows a clear diameter dependence with lower thermal conductivities for smaller diameter wires. This observation suggests that these nanowires could have significantly enhanced thermoelectric figures-of-merit compared to corresponding bulk boron carbides.

Acknowledgements

We appreciate the financial support from the National Science Foundation (CMMI 0748090, 0800366 and 0821604), and the Lockheed Martin Corporation under the program of Engineering & Technology University Research Initiatives. We are grateful to multiuser facilities at UNC Charlotte and Vanderbilt University. We thank the Center for Nanophase Materials Sciences at Oak Ridge National Laboratory for EBID facility. We thank the Cornell Nanofabrication Facilities for microdevice fabrication. We appreciate Dr Weilie Zhou at University of New Orleans and Dr Shuyou Li at Northwestern University for useful discussion on TEM analysis.

Notes and references

1 C. Wood, in *AIP Conf. Proc.*, Albuquerque, New Mexico, 1986, p. 362.
2 T. L. Aselage, in *Mater. Res. Soc. Symp. Proc.*, San Francisco, CA, 1991, p. 145.
3 D. Emin, *J. Solid State Chem.*, 2006, **179**, 2791.
4 H. Werheit, in *25th Int. Conf. Thermoelectr.*, Vienna, Austria, 2006, p. 159.
5 C. Wood, *Rep. Prog. Phys.*, 1988, **51**, 459.
6 H. Werheit, *J. Phys.: Conf. Ser.*, 2009, **176**, 012019.
7 V. I. Matkovich, *Boron and Refractory Borides*, Springer-Verlag, Berlin, 1977.
8 H. Okamoto, *Desk Handbook: Phase Diagrams for Binary Alloys*, ASM International, Materials Park, OH, 2000.
9 G. Chen, M. S. Dresselhaus, G. Dresselhaus, J. P. Fleurial and T. Caillat, *Int. Mater. Rev.*, 2003, **48**, 45.
10 M. S. Dresselhaus, G. Chen, M. Y. Tang, R. Yang, H. Lee, D. Wang, Z. Ren, J.-P. Fleurial and P. Gogna, *Adv. Mater.*, 2007, **19**, 1043.
11 R. Schmechel and H. Werheit, *J. Phys.: Condens. Matter*, 1999, **11**, 6803.
12 I. Gunjishima, T. Akashi and T. Goto, *Mater. Trans.*, 2001, **42**, 1445.
13 H. Werheit, A. Leithe-Jasper, T. Tanaka, H. W. Rotter and K. A. Schwetz, *J. Solid State Chem.*, 2004, **177**, 575.
14 M. S. Dresselhaus, G. Dresselhaus, X. Sun, Z. Zhang, S. B. Cronin and T. Koga, *Phys. Solid State*, 1999, **41**, 679.
15 R. Venkatasubramanian, E. Siivola, T. Colpitts and B. O'Quinn, *Nature*, 2001, **413**, 597.
16 T. C. Harman, P. J. Taylor, M. P. Walsh and B. E. LaForge, *Science*, 2002, **297**, 2229.
17 A. I. Hochbaum, R. Chen, R. D. Delgado, W. Liang, E. C. Garnett, M. Najarian, A. Majumdar and P. Yang, *Nature*, 2008, **451**, 163.
18 B. Poudel, Q. Hao, Y. Ma, Y. Lan, A. Minnich, B. Yu, X. Yan, D. Wang, A. Muto, D. Vashaee, X. Chen, J. Liu, M. S. Dresselhaus, G. Chen and Z. Ren, *Science*, 2008, **320**, 634.
19 A. K. Suri, C. Subramanian, J. K. Sonber and T. Murthy, *Int. Mater. Rev.*, 2010, **55**, 4.
20 M. Carlsson, F. J. Garcia-Garcia and M. Johnsson, *J. Cryst. Growth*, 2002, **236**, 466.
21 R. Z. Ma and Y. Bando, *Chem. Phys. Lett.*, 2002, **364**, 314.
22 F. Xu and Y. Bando, *J. Phys. Chem. B*, 2004, **108**, 7651.
23 W. Q. Han, *Appl. Phys. Lett.*, 2006, **88**, 133118.
24 L. H. Bao, C. Li, Y. Tian, J. F. Tian, C. Hui, X. J. Wang, C. M. Shen and H. J. Gao, *Chin. Phys. B*, 2008, **17**, 4585.
25 J. F. Tian, L. H. Bao, X. J. Wang, C. Hui, F. Liu, C. Li, C. M. Shen, Z. L. Wang, C. Z. Gu and H. J. Gao, *Chin. Phys. Lett.*, 2008, **25**, 3463.
26 X. Y. Tao, L. X. Dong, X. N. Wang, W. K. Zhang, B. J. Nelson and X. D. Li, *Adv. Mater.*, 2010, **22**, 2055.
27 A. Velamakanni, K. J. Ganesh, Y. W. Zhu, P. J. Ferreira and R. S. Ruoff, *Adv. Funct. Mater.*, 2009, **19**, 3926.
28 T. T. Xu, J. G. Zheng, N. Q. Wu, A. W. Nicholls, J. R. Roth, D. A. Dikin and R. S. Ruoff, *Nano Lett.*, 2004, **4**, 963.
29 S. S. Amin, S. Y. Li, J. R. Roth and T. T. Xu, *Chem. Mater.*, 2009, **21**, 763.
30 JCPDS 00-035-0798, 00-044-1206, 04-007-1018, 01-071-0363, 01-074-4876, 03-065-3703.
31 T. T. Xu, A. W. Nicholls and R. S. Ruoff, *Nano*, 2006, **1**, 55.
32 R. S. Wagner and W. C. Ellis, *Appl. Phys. Lett.*, 1964, **4**, 89.
33 K. H. G. Ashbee, *Acta Metall.*, 1971, **19**, 1079.
34 M. A. Kuzenkova, P. S. Kislyi, B. L. Grabchuk and N. I. Bodnaruk, *J. Less Common Met.*, 1979, **67**, 217.

35 I. D. R. Mackinnon, T. Aselage and S. B. Ban Deusen, in *AIP Conf. Proc.*, Albuquerque, New Mexico, 1985, p. 114.
36 M. L. Miller and I. D. R. Mackinnon, in *Mater. Res. Soc. Symp. Proc.*, San Francisco, CA, 1987, p. 133.
37 Y. Li, Y. H. Zhao, W. Liu, Z. H. Zhang, R. G. Vogt, E. J. Lavernia and J. M. Schoenung, *Philos. Mag.*, 2010, **90**, 783.
38 A. Gatti, C. Mancuso, E. Feingold and R. L. Mehan, in *Proceedings of an International Conference on Crystal Growth*, Boston, MA, 1967, p. 317.
39 I. D. R. Mackinnon and K. L. Smith, in *Mater. Res. Soc. Symp. Proc.*, San Francisco, CA, 1987, p. 127.
40 R. Ma and Y. Bando, *Chem. Mater.*, 2002, **14**, 4403.
41 M. Zhu, X. Y. Hu, Y. N. Wei, Y. J. Zhang, X. W. Du and X. Z. Zhang, *J. Cryst. Growth*, 2009, **311**, 3721.
42 X. Fu, J. Jiang, C. Liu and J. Yuan, *Nanotechnology*, 2009, **20**, 365707.
43 J. Jiang, M. H. Cao, Y. K. Sun, P. W. Wu and J. Yuan, *Appl. Phys. Lett.*, 2006, **88**, 163107.
44 R. E. Algra, M. A. Verheijen, M. T. Borgstrom, L. F. Feiner, G. Immink, W. J. P. van Enckevort, E. Vlieg and E. Bakkers, *Nature*, 2008, **456**, 369.
45 X. Fu, J. Jiang, C. Liu, Z. Y. Yu, S. Lea and J. Yuan, *Chin. Phys. Lett.*, 2009, **26**, 086110.
46 Z. Y. Yu, J. Jiang, J. Yuan and J. Zhu, *J. Cryst. Growth*, 2010, **312**, 1789.
47 L. Shi, D. Li, C. Yu, W. Jang, D. Kim, Z. Yao, P. Kim and A. Majumdar, *J. Heat Transfer*, 2003, **125**, 881.
48 D. Li, Y. Wu, P. Kim, L. Shi, P. Yang and A. Majumdar, *Appl. Phys. Lett.*, 2003, **83**, 2934.
49 H. Werheit, *Mater. Sci. Eng., B*, 1995, **29**, 228.

